Journal of Applied Polymer Science

The Role of Crosslinking Treatment on the Pore Structure and Water Transmission of Biocollagenic Materials

Roberto Rodríguez Gil,[1] Begoña Ruiz,[1] Matilde Santiago Lozano,[2] Enrique Fuente[1]

[1]Instituto Nacional del Carbón (CSIC), Francisco Pintado Fe, 26, 33011 Oviedo, Spain

[2]Asociación de Investigación de las Industrias del Curtido y Anexas (AIICA), Avda. Pla de la Massa, s/n, 08700 Igualada, Barcelona, Spain

Correspondence to: E. Fuente (E-mail: enriquef@incar.csic.es)

ABSTRACT: The knowledge of the factors involved in the water transmission through collagen fibrous network of skin and leather is essential in the manufacture of materials that will give improved service and maintain a sufficiently high level of breathability and permeability to assure comfort to the wearer. The study of the structure and connectivity of the pores in the skin and leather is essential since it influences the heat and mass transport processes. This research study focuses on the porous structure and water vapor permeability of animal skin after it has been subjected to different treatments, such as pickling or tanning with chromium salts, or vegetable tannins. The obtained data indicated that surface groups, inorganic matter, and pore size distribution have influence on the water transmission. Water vapor adsorption isotherms showed pickled skin to have a greater adsorption capacity at a higher relative humidity, whereas vegetable-tanned leather was found to be the sample with the lowest adsorption at higher relative humidity probably due to its greater density, lower accessibility of the functional groups, and wider distribution of pore sizes than the other materials. © 2013 Wiley Periodicals, Inc. J. Appl. Polym. Sci. 130: 1812–1822, 2013

KEYWORDS: biomaterials; crosslinking; porous materials; proteins; structure–property relations

Received 5 December 2012; accepted 3 April 2013; Published online 6 May 2013

DOI: 10.1002/app.39365

INTRODUCTION

The most characteristic feature of animal hide is the enrichment of non-collagenous compounds in the papillary layer, so-named because of the presence of hair papillas. This layer contains sweat glands, fat cells, elastin (around the papillas), and muscle fibers located beneath the hide surface that carry out both mechanical and biological functions. In the leather industry, after these compounds have been removed in the beamhouse a very open collagen fibrous structure remains, giving the grain leather surface (the outside of the hide or skin consisting of the pores, wrinkles, and other characteristics which constitute the natural texture of the leather) its characteristic soft feel. Each fiber is composed of elemental fibers and these are made up of groups of collagen fibrils. The structure of the fibrous network is characterized by continual branching. Each elemental fiber branches into two parts and each of these joins with another to form a new elemental fiber strand. It is the branching of the collagen structure that gives the corium layer its woven appearance and the leather its characteristic strength. In making leather, the orientation and thickness of the collagen fiber is of the utmost importance. The structure and connectivity of the pores in the skin influence the heat and mass transport processes associated with both the thermoregulatory function of the organ and the crosslinking of the collagen network in the tanning stage. It is thought that the pore structure of the skin matrix can be used to control adsorption, diffusion phenomena, fluid flow, and thermal conductivity, and its study is very important for understanding the processes of diffusion and/or adsorption through skin in both biological and industrial applications[1–4].

It is an arduous task for the tanner to convert raw hides and skins into leather, which has a three-dimensional matrix with excellent porosity. Many of the properties of leather such as visco-elasticity, plasticity, breathability, and resistance to water are related with its porosity (volume, size, and connectivity between pores and interfibrilar spaces), and a pore size ranging between 7 Å and 150 μm. Leather is a unique material with an ability to breathe through its porous network and readjust to volume fluctuations. Some of its properties are believed to arise from the nature of its collagen fibrous network. For example, the great resistance to flexural fatigue exhibited by leather may be attributed to the ability of individual collagen fibers to reorient themselves under stress. It can be noted the study carried out by Catalina[5] where tanning wastes from leather processing are valorized to tailor-made collagen biopolymers with diverse

shapes (fibers, gels, films, and sponges), which can have important and promising applications in the fields of cosmetics, medicine, or veterinary.

It has been recognized that the transport of moisture under conditions of transient humidity is a key property that influences the dynamic comfort of a leather garment due to the breathability and permeability properties of leather. The amount of moisture that leather adsorbs or loses is determined by temperature, relative humidity, functional surface groups, degree of porosity and the size of the pores, and interfibrilar spaces. Moisture is of great importance because the amount of moisture affects the durability of leather, and in articles such as shoes, gloves, and other garments, the comfort of the wearer. A high moisture content accelerates deterioration and promotes the action of mildew. On the other hand, a small amount of moisture is necessary to keep leather properly lubricated and prevent cracking. From the data obtained from a study of moisture adsorption by leather and untanned hide at various stages of relative humidity, knowledge about the nature, and magnitude of the surfaces may be obtained. Such concepts may be of great value for improving the tanning process, and other related processes such as fat liquoring and dyeing, performing appropriate adjustments to get better functional properties of the final leather.

The characterization of the porous or interfibrilar space inside the collagen matrix was performed by mercury intrusion porosimetry and nitrogen adsorption.[6,7] Mercury injection porosimetry is a commonly used method for the characterization of porous materials and is widely used in industry.[3,6–13] This technique allows the characterization of the porosity of different kinds of materials in order to determine the distribution of porosity over the macropore (pore sizes higher than 50 nm) and mesopore (pores of 2–50 nm) range in addition to other important parameters such as total porosity, total volume of mercury intrusion, bulk density, skeletal density, etc. Mercury porosimetry is a very popular technique because it is relatively straightforward to use and also because it can be used to study a wide range of pore sizes between 360 μm to 6 nm. The measurement range of high-pressure mercury porosimetry is wider than that of nitrogen adsorption (0.3–300 nm). The smallest pores that are outside the range of mercury porosimetry were determined by nitrogen adsorption. Many parameters that describe the pore structure of a sample, for example, pore volume, specific surface area, and pore size distribution can be determined by nitrogen adsorption at 77 K. The information on the porosity of skin and leather gained by these different experimental techniques shows that they complement each other. Furthermore, water vapor adsorption isotherms gave us information of the breathability and permeability of the skin and leather, relating the adsorption capacity with the porosity, inorganic content, and surface chemistry of the biocollagenic materials. This study also employs another technique, scanning electron microscopy which is very useful for the examining and characterizing the surfaces of all kinds of materials.

In the literature, several studies have been carried out on the porous structure of skin and leather,[3,14] in addition to adsorption and transmission of water vapor in leather.[4,15–18] Worthy of special mention are the studies carried out by Fathima et al. regarding the influence of shrinkage on the porous structure of skin and leather by means of mercury intrusion porosimetry, nitrogen adsorption, and scanning electron microscopy,[6,7] the effects of tanning process steps upon pore size distribution,[19] and of crosslinking on the hydration structure of collagen.[20]

MATERIALS AND METHODS

The solid materials used for this research were two pre-tanned skins: a dehydrated and degreased skin (Biomaterial Collagenic Dehydrated, BCD), and a pickled skin (PS); and two tanned skins: a chromium-tanned leather (Wet Blue, CTL), and a vegetable-tanned leather (VTL). BCD was a delimed and bated skin that had been treated with acetone in order to degrease and dehydrate it for conservation; PS was a skin that had been treated with saline solutions and acids in the same bath to prepare it for the tanning operation or for preservation. A sample of skin tanned with vegetable tannins [mimosa (*Acacia dealbata*), quebracho (*Schinopsis lorentzii* and *balansae*), and chestnut (*Castanea sativa*)] was also examined (VTL). Wet-blue leather was a skin that had been tanned with chromium salts (CTL). Pickled skin, wet-blue leather, and skin tanned with vegetable tannins were used as samples of semi-processed leather and they are available on the market. Dehydrated skin was an experimental sample. All the materials were of bovine origin.

The samples that arrived in the form of strips or as one large piece were converted into the appropriate size for the different analyses. In order to obtain a representative sample of the precursor for chemical analysis they were ground to a very fine particle size. For the mercury porosimetry, nitrogen adsorption at −196°C, water-vapor sorption at 25°C, and scanning electron microscopy experiments, small pieces of skin with maximum measurements of up to 1 × 1 × 0.2 cm were used. Prior to their analysis the samples were degassed under vacuum at 50°C overnight up to constant weight so as to remove any adsorbed moisture and/or gases. A low temperature was chosen so as not to denature the protein of the skin, and prevent the shrinkage of the skin. The porosity measurements have to be done on dried sample because the porosity has to be empty for filling with nitrogen (nitrogen isotherm at −196°C), mercury (Mercury Intrusion Porosimetry), or water-vapor (water-vapor sorption at 25°C).

Chemical Characterization

A proximate and ultimate analysis of the samples was conducted following the procedures usually applied to coals. The ash content was determined according to norm UNE 32004. The ultimate analysis was carried out on a LECO CHN-2000 and LECO Sulphur Determination S-144-DR instrument. The oxygen content was calculated by difference.

Textural Characterization

Mercury Porosimetry. Mercury porosimetry was carried out on a Micromeritics AutoPore IV 9500 Series apparatus, which provided a maximum operating pressure of 227 MPa. The mercury porosimetry was conducted as follows: the sample was weighed in a penetrometer, degassed and then filled with distilled mercury at a low pressure. The mercury was then subjected to different pressures and the corresponding volumes of the

intruded mercury in the samples were determined. The pore diameter was calculated from the pressure values, the surface tension of the mercury and the wetting angle using the Washburn equation,[21] assuming a mercury surface tension of 480 N m^{-122} and a mercury contact angle of 140°. The following parameters were calculated: bulk and skeletal densities (ρ_b and ρ_s, respectively), the specific total pore volume corresponding to the intruded volume of mercury at maximum pressure (V_T), the porosity (ε), and the pore size distribution.

From the skeletal (ρ_s) and bulk (ρ_b) densities the total pore volume (V_T) was calculated from:

$$V_T = (1/\rho_b - 1/\rho_s)$$

and the open porosity, ε, from:

$$\varepsilon = (1 - \rho_b/\rho_s) \times 100$$

Nitrogen Adsorption Isotherms. Nitrogen adsorption isotherms were performed at −196°C in a Micromeritics ASAP 2420 automatic apparatus. The isotherms were used to calculate the specific surface area S_{BET}, parameter C, the volume of the monolayer and total pore volume, V_{TOT}, at a relative pressure of 0.95. The pore size distributions, i.e., microporosity and mesoporosity, were obtained by applying the density functional theory (DFT) model to the N_2 adsorption data, assuming slit-shaped pore geometry.[23]

SEM-EDX. The materials were examined using a Scanning Electron Microscope (ZEISS Model DMS-942) equipped with an Energy-Dispersive X-Ray analyzing system (Link-Isis II). Iridium was present because the samples had been metalized for examination by SEM-EDX so as to avoid the accumulation of electric charge on the surface and to make the samples electrically conductive.

Water-Vapor Sorption Isotherm at 25°C. The moisture adsorption isotherms of the samples were determined at 25°C for water activity (a_w) from 0 to 1. Water activity was evaluated by means of a Hydrosorb HS-12-HT model instrument (Quantachrome Instruments). The equilibrium moisture content was expressed as grams per g of dry solid.

RESULTS AND DISCUSSION

Chemical Characterization

Figure 1 shows the results of the proximate and ultimate analysis of the samples. The results of the chemical analysis of these materials reveal a low ash content; being wet blue-CTL the material with highest value in mineral matter (ash: 9.15%), which is attributed to chemical reagents used in the process of tanning; the dehydrated skin has the lowest ash content, 1.23%. All of the samples contain a high carbon content in the range of 40–50% and a substantial nitrogen content with values up to 18% (17.89 for BCD). Similar results for the chemical composition of tannery wastes of vegetable-tanned leather and chromium-tanned leather have been reported by Cem Kantarli et al.,[24] Yilmaz et al.,[25] Oliveira.[26]

The vegetable-tanned leather shows a lower nitrogen content (8.33%) and a higher oxygen content (29.58%) than the other materials because of the large amount of vegetable tannins needed for the tanning process (Figure 1). In the leather obtained at the end of the process, vegetable tannins are present in concentrations of around 30%.

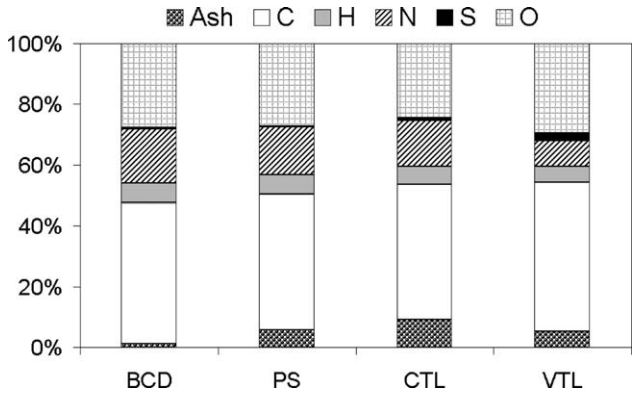

Figure 1. Proximate and ultimate analysis of the samples (units: wt %, db).

The chemical composition of these materials makes them suitable bioprecursors for obtaining activated carbons. Several studies on the physical activation of tanned leather wastes with CO_2[24–28] or steam,[29] and on the chemical activation of leather shaving wastes[24,30] and leather buffing dust wastes[31] are reported in the literature. Gil has published several works related to the chemical activation of vegetable-tanned leather solid wastes by means of alkaline hydroxides and carbonates.[32–36] Furthermore, the high nitrogen content of these materials makes them very useful for producing activated carbons that can be employed in H_2S and SO_2 adsorption[37] or CO_2 capture.[38,39]

Textural Characterization

Mercury Intrusion Porosimetry. Table I shows the results of the textural characterization of the samples by mercury porosimetry. The total intrusion volume, total surface area, median pore diameter (volume), median pore diameter (area), average pore diameter ($4V/A$), bulk density at 0.0045 MPa, bulk density at 0.1013 MPa, skeletal density at 227 MPa, and porosity were determined by mercury porosimetry.

The results vary widely for the different samples. The materials present a total pore volume of mercury intrusion of between 0.7 and 1 mL g^{-1}, except for pickled skin which has the lowest value (0.14). This is attributed to the reduction or blockage of porosity resulting from the chemical treatment to which the pickled skin was subjected. Such preservation treatment protects the skin against external agents. The porosity values—17% for pickled skin and 50–61% for the other samples—confirm the above findings. The bulk density value recorded at a pressure of 0.0045 MPa for pickled skin, 1.19 mL g^{-1}, was twice as high as that of the other samples, i.e., around 0.6 mL g^{-1}. All the results suggest that the chemical treatment to which the pickled skin was subjected reduced its porosity.

There are numerous studies in the literature on the pore structure of different materials. Fathima et al.[7] have studied the influence of crosslinking agents on the pore structure of skin. They also studied the effect of thermal shrinkage on the pore structure of native skin and chromium and vegetable treated

Table I. The Intrusion Data From the Mercury Porosimetry Technique

	Dehydrated skin	Pickled skin	Wet blue leather	Skin tanned with vegetable tannins
Total intrusion volume, V_T, (mL/g)	0.992	0.141	0.671	0.682
Total surface area (m^2/g)	10.1	5.6	3.7	20.9
Median pore diameter (Volume) (nm)	3251.5	1431.9	8585.4	691.1
Median pore diameter (Area) (nm)	26.0	10.4	34.2	33.8
Average pore diameter (4V/A) (nm)	392.0	100.4	727.8	130.6
Bulk density at 0.0045 MPa, ρ_b, (g/mL)	0.60	1.19	0.74	0.75
Bulk density at 0.1013 MPa, ρ_b, (g/mL)	0.63	1.23	0.82	0.81
Skeletal density at 227 MPa, ρ_s, (g/mL)	1.46	1.43	1.46	1.55
Porosity, ε, (%)	59.2	16.8	49.5	51.4

skin. They observed that the percentage reduction in porosity was greater in the vegetable skin than in the chromium treated sample.

The cumulative pore volume and the pore volume size distribution obtained by mercury porosimetry for each sample are presented in Figure 2. The cumulative pore volume represents the total volume contained in pore sizes of that diameter or less. The pore volume size distribution curve represents the pore volume in function of pore size, commonly is given as percentage or a derivative, and highlights the differences in the pore sizes of the samples.

The mercury porosimetry measurements show a significant macroporosity development in the case of the dehydrated skin. The macropore volume development in this sample was more than seven times greater than that of the pickled skin as can be seen in the cumulative pore volume in Figure 2. The latter was subjected to chemical treatment to reduce its porosity for purposes of preservation. In contrast, wet-blue leather (the skin

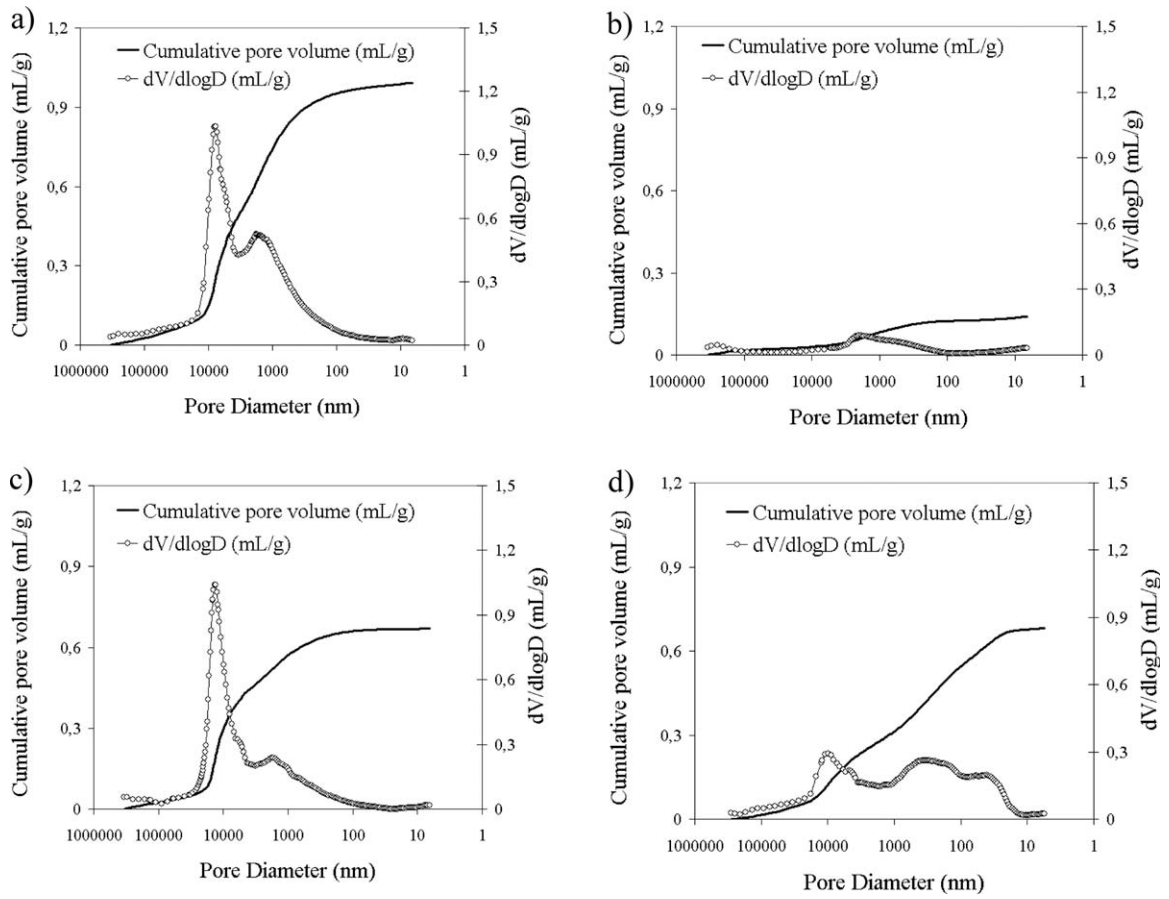

Figure 2. Cumulative pore volume and pore volume size distribution by mercury porosimetry for the samples of this research: (a) dehydrated skin, (b) pickled skin, (c) wet blue leather, and (d) skin tanned with vegetable tannins.

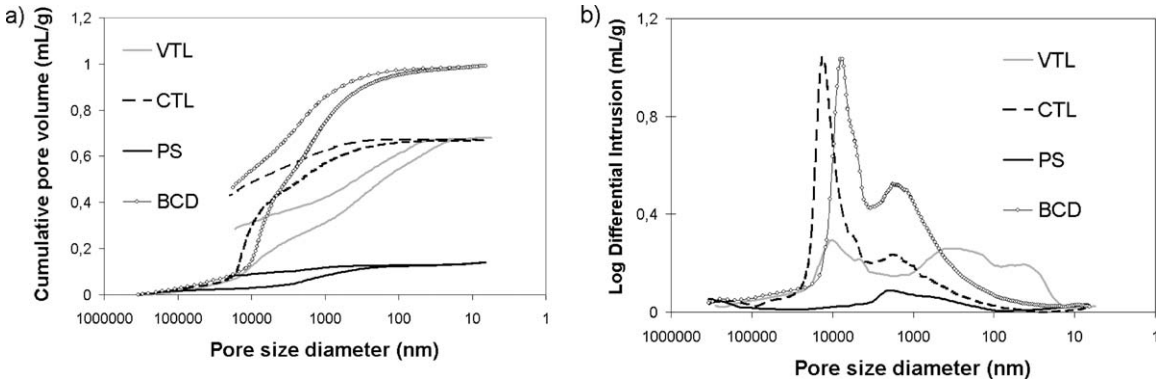

Figure 3. (a) Mercury intrusion and extrusion curves. (b) Pore size distribution by mercury intrusion porosimetry.

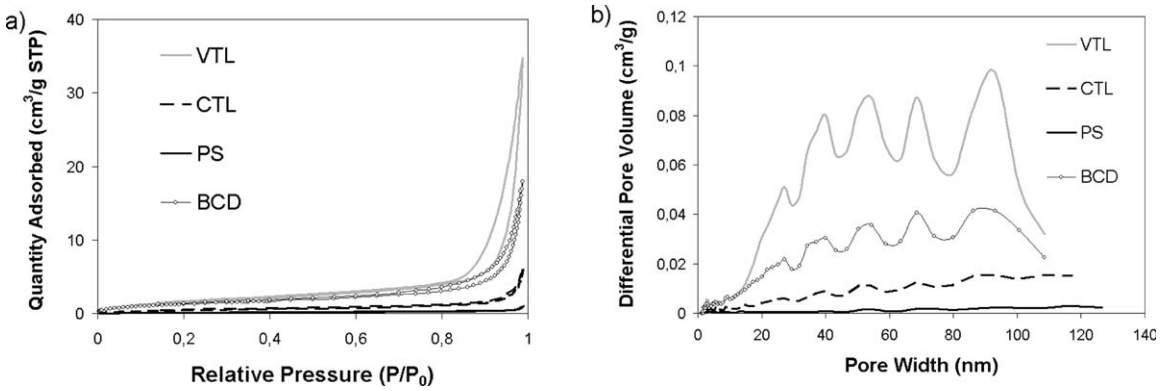

Figure 4. (a) Nitrogen adsorption isotherms at −196°C. (b) Pore size distribution by DFT.

tanned with chromium salts) and the skin tanned with vegetable tannins showed a moderate macroporous development. It is evident from these results that in general the development of macroporosity also depends on the tanning agent. There are numerous studies on the macropore volume development of different materials. Ruiz et al.[10] studied the effect of oxidation on macropore volume development in carbonized coals. Fathima et al. studied the porosity of native and shrunken samples of skin by means of the cumulative intrusion volume of mercury. It can be seen from their results that the cumulative intrusion of mercury is greater in the case of native skin than in that of the shrunken samples.[7]

Table II. Equivalent Specific Surface Area-BET, Parameter C_{BET}, Monolayer volume (Q_m), Total Pore Volume at P/P_0: 0.99 and P/P_0: 0.95, and Mesopore Volume of the Materials

	BCD	PS	CTL	VTL
Surface area-BET (m^2/g)	4.9	0.7	1.8	6.5
C_{BET}	32.0	5.6	18.2	22.5
Q_m (cm^3/g STP)	1.13	0.16	0.42	1.48
V_t, P/P_0: 0.95 (cm^3/g)	0.011	0.001	0.003	0.017
V_t, P/P_0:0.99 (cm^3/g)	0.030	0.002	0.010	0.057
V_{me}[a] (2–50 nm)	0.016	0.001	0.005	0.031

[a] Data from DFT.

The pore volume size distribution highlights the differences in the pore sizes of the samples (Figure 2). Dehydrated skin and wet blue leather show bimodal volume pore size distributions with two maximum peaks at 7500–1500 nm and 13,000–1700 nm, respectively. The skin tanned with vegetable tannins shows a wide distribution pore size with three maxima at approximately 10,000, 300, and 40 nm and it is the only material that presents narrower pores between 100 and 10 nm. Finally, pickled skin exhibits the lowest volume mercury intrusion with a maximum at 2000 nm on the pore size distribution curve. The chemical treatment to which this sample was subjected seems to have eliminated macropores or interfibrilar spaces larger than 5 microns.

Figure 3 shows the mercury intrusion and extrusion curves [Figure 3(a)] and pore size distributions [Figure 3(b)] for all the samples with comparative purposes.

Figure 3(a) demonstrates BCD is the sample with a highest intrusion values whereas PS is the material with lowest intrusion values. All the samples showed a hysteresis loop due to the penetration of mercury into pores and interfibrilar spaces where it remains trapped. Figure 3(b) shows the different pore size distributions of the materials: bimodal (BCD and CTL), wide distribution (VTL) and low volume mercury intrusion (PS).

Nitrogen Adsorption Isotherm at −196°C. Nitrogen adsorption analysis confirms and complements the results obtained by mercury porosimetry (Figure 4). The nitrogen isotherms are of

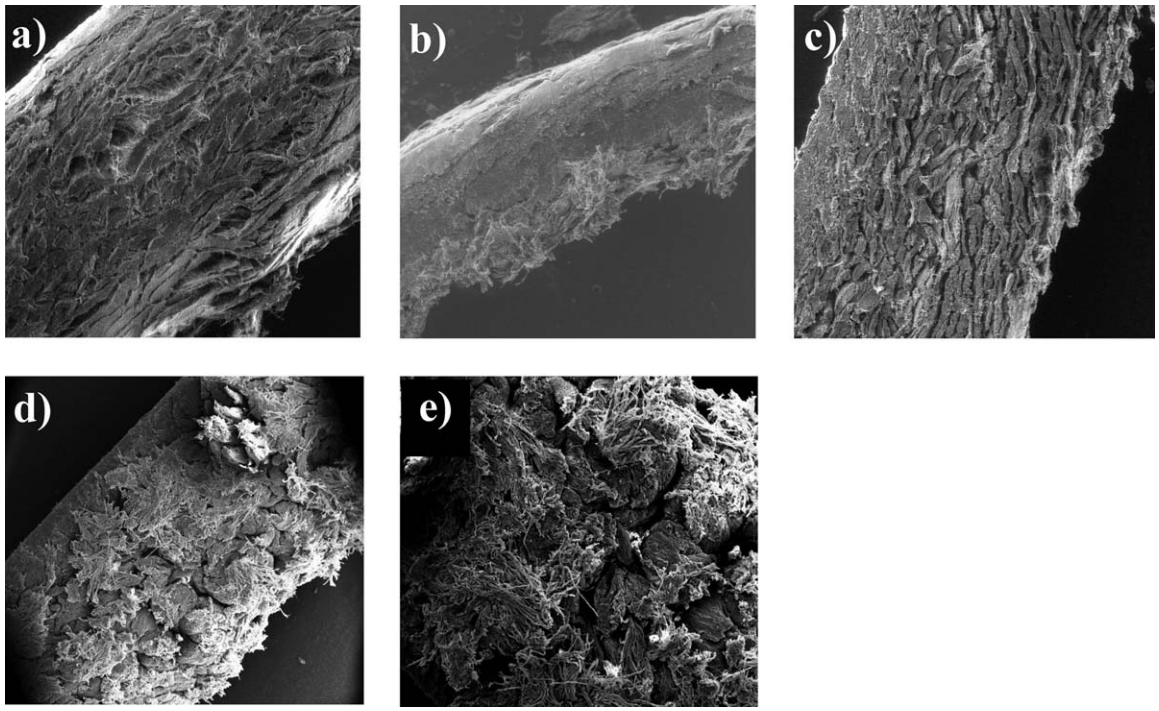

Figure 5. SEM cross-section micrographs of the materials: (a) BCD (100×); (b) PS (100×); (c) CTL (100×); (d) VTL (50×); (e) VTL (100×).

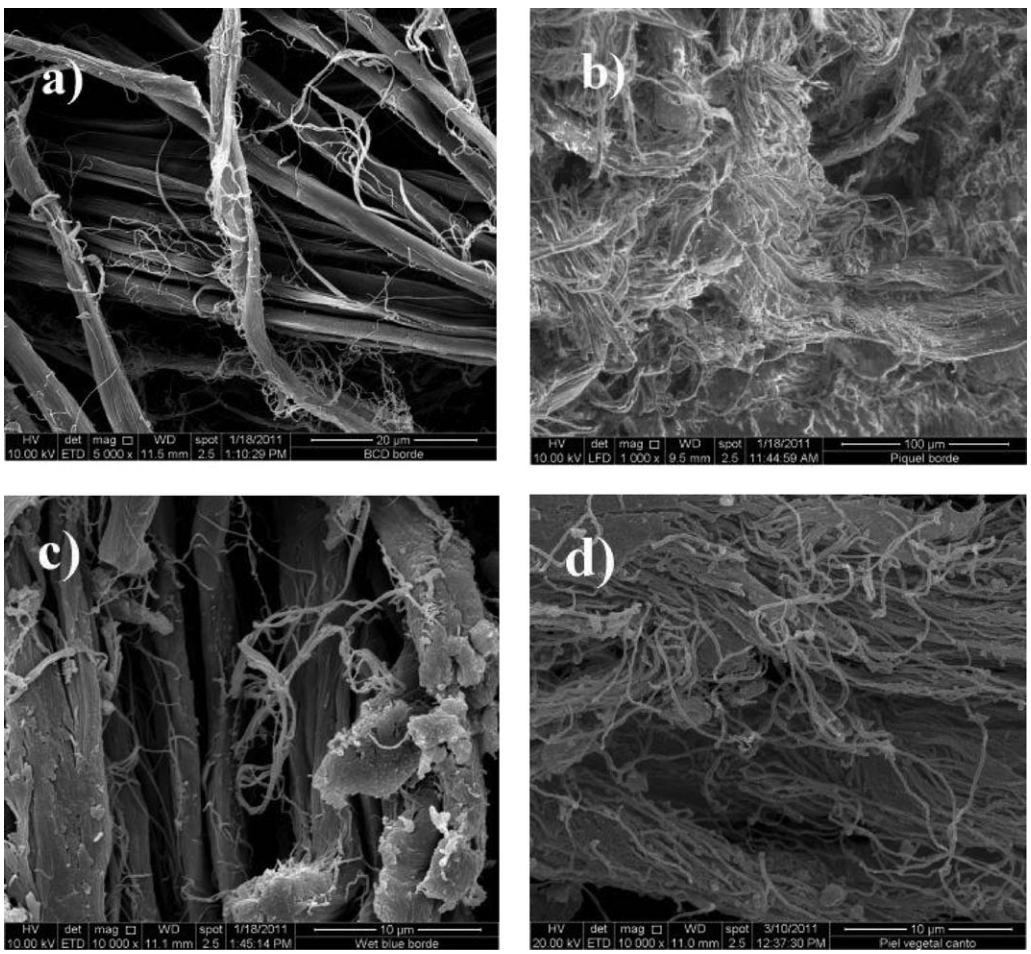

Figure 6. SEM cross-section micrographs of the materials: (a) BCD (5000×); (b) PS (1000×); (c) CTL (10,000×); (d) VTL (10,000×).

Applied Polymer SCIENCE

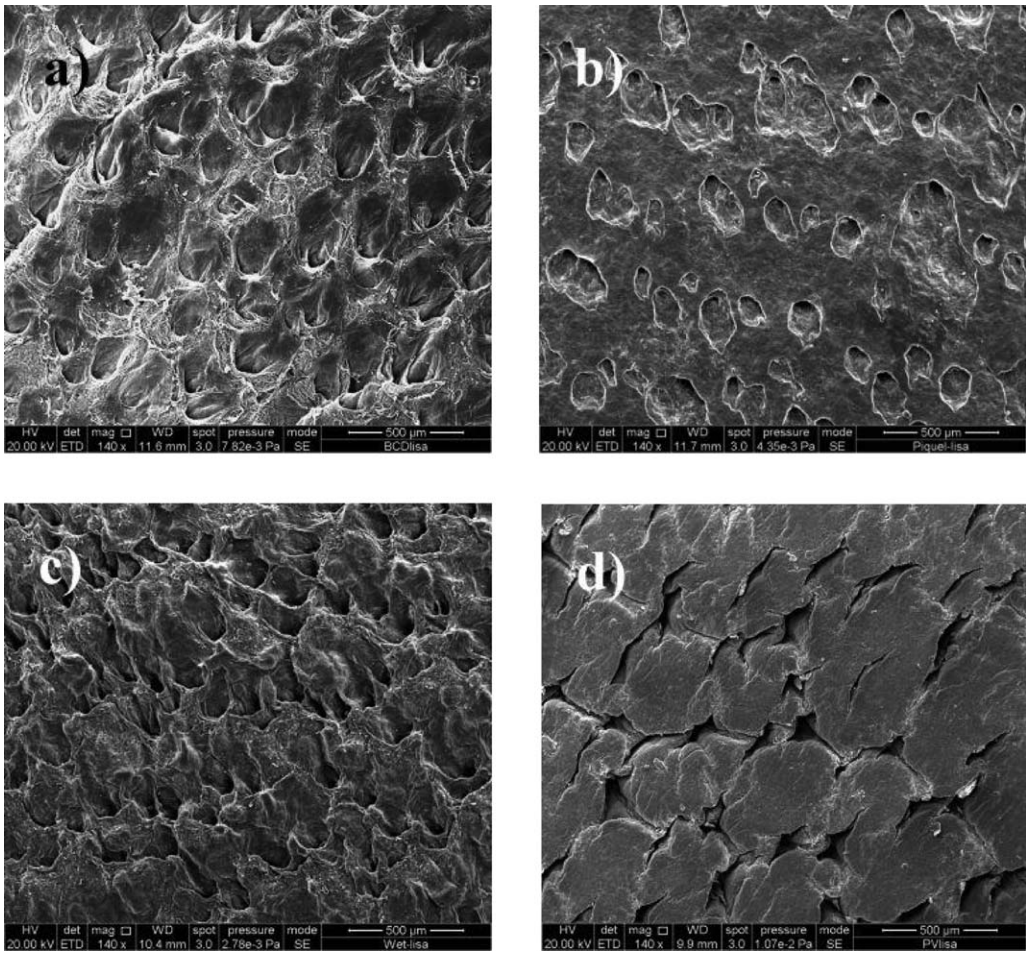

Figure 7. SEM micrographs of the grain surface of the materials (140×): (a) BCD; (b) PS; (c) CTL; (d) VTL.

type III which is typical of non-porous or macroporous solids. This type of isotherm is convex to the P/P_0 axis over its entire range and indicates that the attractive adsorbate–adsorbent interactions are relatively weak and that the adsorbate–adsorbate interactions play an important role. Hysteresis loop of type H3 for VTL and BCD is observed, indicating a condensation phenomenon. This hysteresis loop does not exhibit any limiting adsorption at high P/P_0 and is normally observed with aggregates of plate-like particles that give rise to slit-shaped pores.[40,41] The desorption branch contains also a steep region associated with a (forced) closure of the hysteresis loop, which was attributed to the so-called tensile strength effect. VTL presents the highest values for the equivalent specific surface area-BET (6.5 m^2/g) and the total pore volume at P/P_0: 0.95 (V_t: 0.017 cm^3/g), as seen in Table II.

The parameter C_{BET} provides an indication of the strength of the adsorbent–adsorbate interactions but cannot be used to quantitatively calculate the enthalpy of adsorption. The decrease in C_{BET} value indicates that the net heat of adsorption in the case of the skin matrix decreases on tanning. The heat of nitrogen adsorption is probably influenced by changes in the surface and by the level of hydrophobicity.

Information about structural changes in the samples can be obtained by analyzing the pore size distributions of the native and tanned samples [Figures 3(b) and 4(b)]. All the materials have mainly meso and macroporosity. VTL has a higher mesoporosity and macroporosity of small pore size than the other materials, as can also be observed by mercury porosimetry. The mesoporosity and macroporosity of small pore size decrease in the following order: VTL > BCD > CTL > PS, with PS showing almost negligible amounts. CTL presents the largest pore size as can be observed by mercury porosimetry, whereas PS shows no significant porosity in any of the porosity ranges.

SEM-EDX. Figure 5 shows SEM cross-section micrographs of the samples at several magnifications. The dehydrated collagenic biomaterial presents a compact and dense fibrous structure, where the spaces between fibers have been caused by dehydration and degreasing with acetone [Figure 5(a)]. The spaces are suitable for subsequent treatments such as pickling, tanning, etc., for which the solutions need to penetrate into the fibrous structure. The micrograph of the pickled skin [Figure 5(b)] shows that the spaces seem like they were filled with the acid and salts added to the skin matrix to prepare it for the tanning process.

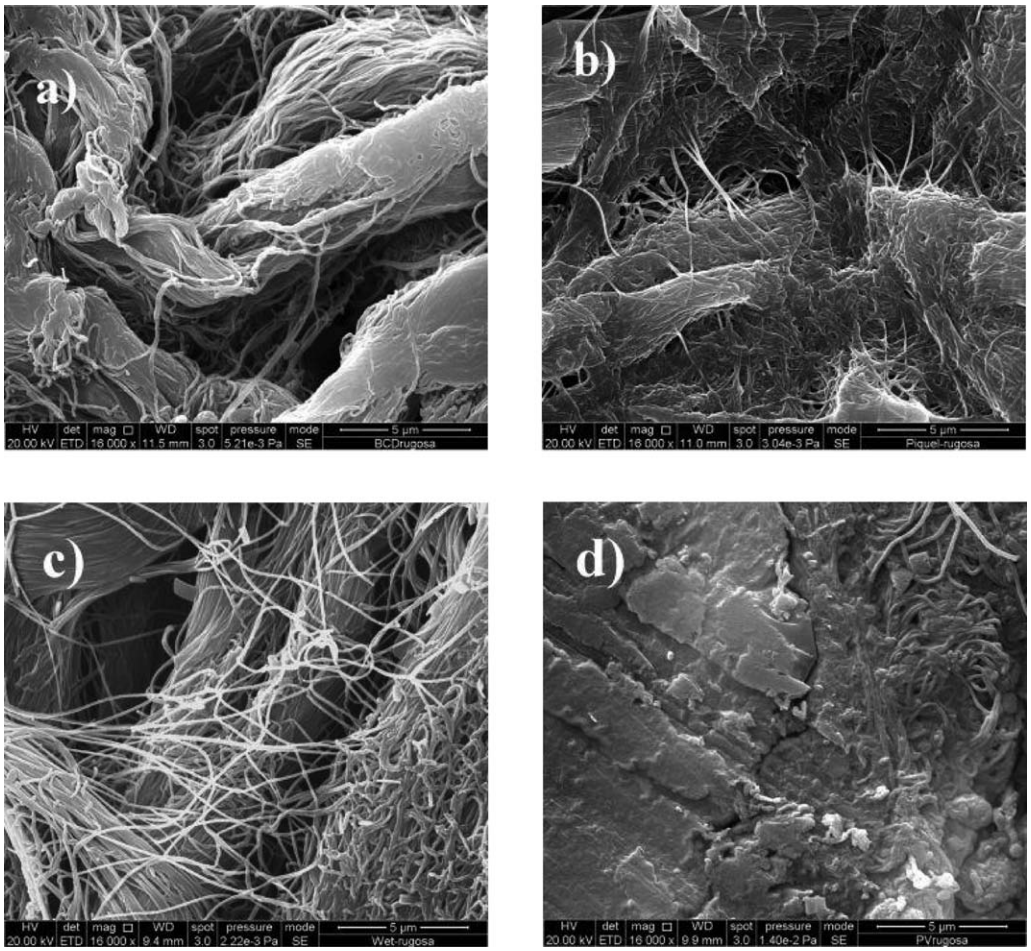

Figure 8. SEM micrographs of the internal surface of the materials (16,000×): (a) BCD; (b) PS; (c) CTL; (d) VTL.

Vegetable tanning results in the filling up of void spaces[42] accompanied by the formation of hydrogen bonds and the coating of fibers [Figure 5(d,e)], whereas chrome tanning is a non-filling type of tanning process, leading to coordinate covalent crosslinking, where the fibrous structure does not show much compactation [Figure 5(c)],[43,44] so the density of vegetable-tanned leather will be higher than other tanned skins.

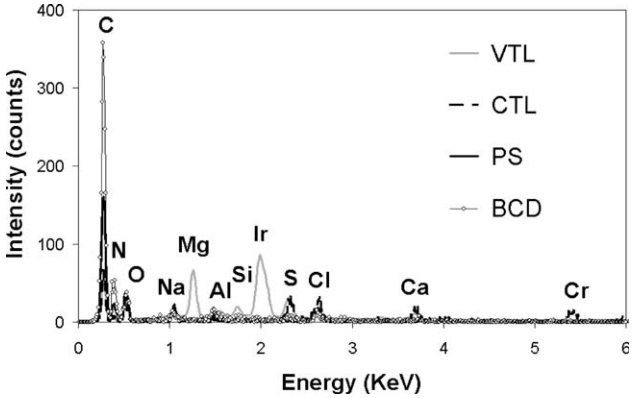

Figure 9. EDX spectra of the skin materials.

Figure 6 shows the micrographs of the materials taken at higher magnification in order to relate the results from the study of mercury intrusion volume and nitrogen adsorption with the porosity or interfibrilar spaces of the samples under study. BCD shows the elemental fibers that constitute the collagen network, together with the fibrils that constitute the elemental fibers [Figure 6(a)]. It can be seen that PS does not have any significant porosity [Figure 6(b)]. BCD is the material with the largest porosity [Figure 6(a)]. The void spaces in VTL are filled by tannins which are also coating the fibers [Figure 6(d)]. CTL is illustrative of a non-filling type of tanning process with larger spaces between the fibers than in the case of VTL [Figure 6(c)].

Figure 7 shows the grain surface of the different materials. The tanned materials of bovine origin present a similar pore shape. These pores are a consequence of the removal of surface hairs from their roots due to the stages of dehairing, liming, deliming, and bating.

Figure 8 contains micrographs of the internal surfaces of the materials. BCD shows spaces between the fibers caused by dehydration and degreasing with acetone, resulting in a high porosity [Figure 8(a)]. Figure 8(b) also shows the low porosity of PS probably because the gaps are filled by the acid and salts added in the pickling process. VTL reflects a lower porosity than CTL

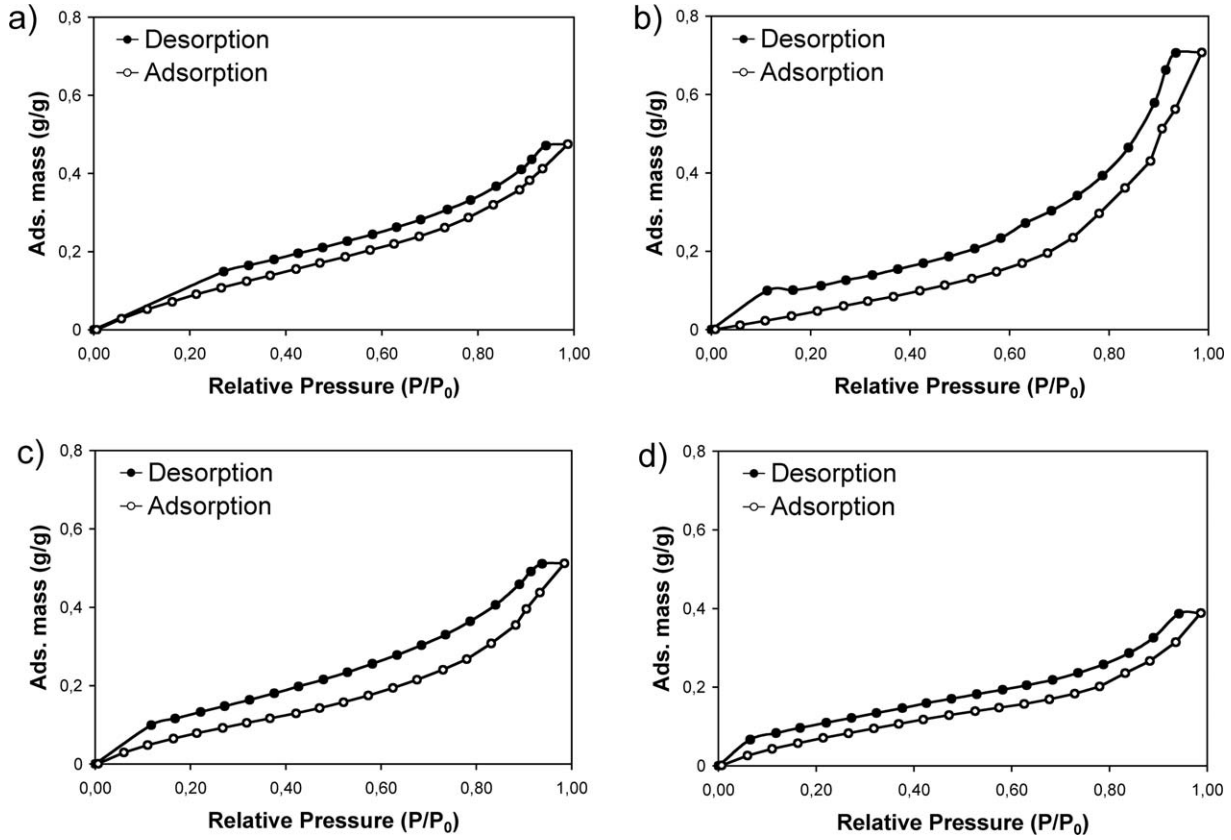

Figure 10. Water vapor adsorption isotherms of the materials: (a) BCD; (b) PS; (c) CTL; (d) VTL.

because the void spaces are filled and the fibers are coated by vegetable tannins.

Figure 9 shows the EDX spectra of the samples. It can be seen that structural carbon, nitrogen, and oxygen are present in all the samples. Sulphur is present probably in the form of sulfates such as magnesium sulfate which is used in vegetable-tanned leather production as a co-adjuvant (the addition of magnesium sulfate makes the leather softer, promotes the fixation of tannin to the skin, and increases the weight). The materials may also contain small amounts of sulfide, calcium hydroxide, sodium chloride, potassium chloride, carbonates, etc, due to the chemical agents employed in the tanning process. Heavy metals are absent in the tanned leathers except in the case of CTL which contains chromium, originating from the tanning agent.

Water Vapor Adsorption Isotherm at 25°C. A knowledge and understanding of sorption isotherms is essential in science and technology for the design and optimization of drying equipment and packages, for predicting quality, stability, shelf-life, and for calculating moisture changes that may occur during storage. Several preservation processes have been developed in order to prolong the shelf-life of products. These involve reducing the availability of water to micro-organisms and preventing certain chemical reactions. The shape of an isotherm can reflect the way water is bound to the system. Weaker water molecule interactions generate greater water activity. The product then becomes more unstable. Water activity depends on the composition, temperature, and physical state of the compounds.

It is well known (Bull in 1944,[45] and Dole and McLaren in 1947[46] that water is related to collagen in four different processes, which are dependent upon vapor pressure (relative humidity) (Kozlov and Burdygina in 1988[47]. A specific amount of water is necessary for the molecular stability of the tropocollagen structure. The role that water plays in ensuring stability is demonstrated in the region from <1% to 25% of relative humidity. This water, bound by high-energy sorption centers, occurs inside the collagen triple helix and plays a stabilizing role through intramolecular hydrogen bonds that form a monomolecular layer. From approximately 25% to 60% of relative humidity, the water is absorbed onto hydrophilic sites in proteins. This water, which is directly bound to the protein (both inside and outside helical fragments) by H-bonds and is considered as structural water, also contributes substantially to the stabilization of the collagen helical structure. The amount of water present in the collagen probably corresponds with the amount contained in the so-called monomolecular layer. From 60% to 90% water is absorbed on polymolecular layers or entrapped in the material by capillary, Van der Waals forces, etc. The monomolecular layer is transformed into a polymolecular layer, which covers the triple helix structure. Above 90% R.H. (near saturation) free water exists in the structure. Water molecules in this region are much less strongly bound than in the previously

mentioned regions. This fraction of water is available for the growth of mold or the dissolution of soluble solutes.

Furthermore, the tensile properties of collagen are dependent of moisture content. Water sorption is also intimately involved in dimensional changes and the swelling of the material.

Figure 10 shows the water vapor adsorption/desorption isotherms at 25°C of the samples. The isotherms are composed of adsorption (down) and desorption branch (up). Hysteresis loops are present in all the samples probably because the adsorbate penetrates pores with narrow entrances where it remains trapped, i.e., factors that could involve the ink bottle theory, the molecular shrinkage theory, the capillary condensation, or the swelling fatigue theory. The first adsorption region ranges from a relative pressure of 0–0.2. It can be seen that the sample with the highest adsorption in the first region is BCD [Figure 10(a)] while the sample with the lowest adsorption is PS [Figure 10(b)]. This is because of the greater accessibility of the pore structure (high porosity and surface area-BET) and the presence of functional groups on the surface of the material (BCD), that facilitate the formation of H-bonds between the functional groups of the aminoacids of the collagen (–OH, –COOH, –CO–NH, and NH_2) and the water. The second region ranges from a relative pressure of 0.2–0.6 and is considered as structural water. The third region (P/P_0: 0.6–0.9) is characterized by the high amount of water vapor adsorbed by PS [Figure 10(b)] followed by CTL [Figure 10(c)]. BCD and VTL also adsorb water vapor in this region but to a lesser extent. The last region (P/P_0: $>$ 0.9) shows a similar adsorption trend to the third region. The water adsorbed in these regions is more available and therefore the samples with a higher degree of adsorption (PS) are more permeable and unstable, favoring the growth of mold, and the dissolution of soluble solutes. The high adsorption of PS in these regions is ascribed to the presence of salts and acids (hygroscopic and deliquescent materials) used in the pickling process. VTL is the material with the lowest adsorption at higher relative humidity probably due to its greater density, lower accessibility of the functional groups and wider distribution of pore sizes than the other materials, and therefore is the most suitable for applications such as shoe soles [Figure 10(d)].

CONCLUSIONS

The mercury intrusion porosimetry, nitrogen adsorption at −196°C and scanning electron microscopy are proposed as suitable techniques for the characterization of the porosity of these kinds of materials and they have shown how different skin treatments cause changes to the porous structure, being essentially macroporous materials.

Water vapor adsorption provides information about the functional surface groups and water transmission of the samples. The obtained data indicated that degreased and dehydrated skin has the highest water vapor adsorption at low relative humidity (<60%) because of the active sites (hydrophilic sites in proteins) and its bimodal pore size distribution. Tanned skins presented nearly the same adsorption in this region, while pickled skin had the least adsorption due to its low porosity. Pickled Skin, with great content of hygroscopic and deliquescent matter, noted for its high adsorption from 60% of relative humidity. Chromium Tanned Leathers, which presented an increase in pore size, kept a high level of water vapor transmission necessary to make the wearer comfortable, while Vegetable Tanned Leather emphasized by a wider pore size distribution with presence of a certain amount of mesopore volume and macropores of small pore size, being the material with lowest adsorption at higher relative humidity and suitable for shoe soles. Thus, we propose the water vapor adsorption isotherm as a suitable technique for the study of breathability and permeability in skins and leathers.

ACKNOWLEDGMENTS

The authors are grateful to Miquel Farrés Rojas S.A. for providing financial support through the PETRI project (MICINN, PET2007_0421_02).

REFERENCES

1. Strombert, R. R.; Swerdlow, M. *J. Am. Leather Chem. Assoc.* **1955**, *50*, 336.
2. Carter, T. J.; Kanagy, J. R. *J. Am. Leather Chem. Assoc.* **1954**, *49*, 23.
3. Kanagy, J. R. *J. Am. Leather Chem. Assoc.* **1963**, *58*, 524.
4. Kanagy, J. R.; Vickers, R. *J. Am. Leather Chem. Assoc.* **1950**, *45*, 211.
5. Catalina, M.; Cot, J.; Balu, A. M.; Serrano-Ruiz, J. C.; Luque, R. *Green Chem.* **2012**, *14*, 308.
6. Fathima, N. N.; Dhathathreyan, A.; Ramasami, T. *Biomacromolecules* **2002**, *3*, 899.
7. Fathima, N. N.; Dhathathreyan, A.; Ramasami, T. *Colloids Surf. B* **2007**, *57*, 118.
8. Moscou, L.; Lub, S. *Powder Technol.* **1981**, *29*, 45.
9. Ruiz, B.; Parra, J. B.; Pajares, J. A.; Pis, J. J. *J. Anal. Appl. Pyrol.* **2001**, *58–59*, 873.
10. Ruiz, B.; Parra, J. B.; Pajares, J. A.; Pis, J. J. *J. Anal. Appl. Pyrol.* **2006**, *75*, 27.
11. Spitzer, Z. *Powder Technol.* **1981**, *29*, 177.
12. Westermarck, S.; Juppo, A. M.; Kervinen, L.; Yliruusi, J. *Eur. J. Pharm. Biopharm.* **1998**, *46*, 61.
13. Whittemore, O. J. *Powder Technol.* **1981**, *29*, 167.
14. Kanagy, J. R. In Biophysical Properties of the Skin; Elden, H. R., Ed.; Wiley: New York, **1971**; pp 373–391.
15. Green, R. W. *Trans. R. Soc. N. Z.* **1948**, *77*, 24.
16. Gulbiniene, A.; Jankauskaite, V.; Alisauskaite, R. *Mater. Sci.* **2003**, *9*, 275.
17. Kanagy, J. R. *J. Res. Natl Bur. Stand.* **1947**, *38*, 119.
18. Kanagy, J. R. *J. Res. Natl Bur. Stand.* **1950**, *44*, 31.
19. Fathima, N. N.; Pradeep Kumar, M.; Raghava Rao, J.; Nair, B. U. *Thermochim. Acta* **2010**, *501*, 98.
20. Fathima, N. N.; Baias, M.; Blumich, B.; Ramasami, T. *Int. J. Biol. Macromol.* **2010**, *47*, 590.
21. Washburn, E. W. *Phys. Rev.* **1921**, *17*, 273.

22. Ritter, H. L.; Drake, L. C. *Ind. Eng. Chem. Anal. Ed.* **1945**, *17*, 782.
23. Jagiello, J.; Thommes, M. *Carbon* **2004**, *42*, 1227.
24. Kantarli, I. C.; Yanik, J. *J. Hazard. Mater.* **2010**, *179*, 348.
25. Yilmaz, O.; Cem Kantarli, I.; Yuksel, M.; Saglam, M.; Yanik, J. *Resour. Conserv. Recycl.* **2007**, *49*, 436.
26. Oliveira, L. C. A.; Coura, C. V. Z.; Guimaraes, I. R.; Gonçalves, M. *J. Hazard. Mater.* **2011**, *192*, 1094.
27. Martinez-Sanchez, M. A.; Orgiles-Barcelo, C.; Martin-Martinez, J. M.; Rodriguez-Reinoso, F. In Pyrolysis and Gasification; Ferrero, G. L., Maniatis, K., Buekens, A., Bridgewater, A. V., Eds.; Elsevier: New York, **1989**; pp 439–443.
28. Oliveira, L. C. A.; Guerreiro, M. C.; Gonçalves, M.; Oliveira, D. Q. L.; Costa, L. C. M. *Mater. Lett.* **2008**, *62*, 3710.
29. Putshak'a, J. D.; Akpabio, I. O. *J. Am. Leather Chem. Assoc.* **2010**, *105*, 313.
30. Gil, R. R.; Girón, R. P.; Ruiz, B.; Lozano, M. S.; Martín, M. J.; Fuente, E. In Book of Abstracts, RECIMAT'09. 1st Spanish National Conference on Advances in Materials Recycling and Eco-Energy, Madrid, **2009**; p 25.
31. Sekaran, G.; Shanmugasundaram, K. A.;Mariappan, M. *J. Hazard. Mater.* **1998**, *63*, 53.
32. Gil, R. R.; Girón, R. P.; Lozano, M. S.; Canals Batlle, C.; Anfruns, A.; Martín, M. J.; Ruiz, B.; Fuente, E. In Book of Abstracts, X Reunión del Grupo Español del Carbón, Girona, **2010**; pp 127–128.
33. Gil, R. R.; Girón, R. P.; Lozano, M. S.; Fuente, E.; Ruiz, B. In Book of Abstracts, XI Reunión del GEC, Badajoz, **2011**; pp 197–198.
34. Gil, R. R.; Girón, R. P.; Lozano, M. S.; Ruiz, B.; Fuente, E. In Book of Abstracts, XI Reunión del GEC, Badajoz, **2011**; pp 195–196.
35. Gil, R. R.; Girón, R. P.; Lozano, M. S.; Ruiz, B.;Fuente, E. In Book of Abstracts, 37th Reunión Ibérica de Adsorción, Sevilla, **2012**; pp 51–52.
36. Gil, R. R.; Girón, R. P.; Ruiz, B.; Lozano, M. S.; Martín, M. J.; Fuente, E.; Castell, J. C.; Adzet, J. M. A. In Book of Abstracts, XXXI IULTCS Congress, Valencia, **2011**; p E35.
37. Bagreev, A.; Bashkova, S.; Bandosz, T. J. *Langmuir* **2002**, *18*, 1257.
38. Pevida, C.; Plaza, M. G.; Arias, B.; Fermoso, J.; Rubiera, F.; Pis, J. *J. Appl. Surf. Sci.* **2008**, *254*, 7165.
39. Shafeeyan, M. S.; Daud, W. M. A. W.; Houshmand, A.; Shamiri, A. *J. Anal. Appl. Pyrol.* **2010**, *89*, 143.
40. Sing, K. S. W.; Everett, D. H.; Haul, R. A. W.; Moscou, L.; Pierotti, R. A.; Rouquerol, J.; Siemieniewska, T. *Pure Appl. Chem.* **1985**, *57*, 603.
41. Boer, J. H. D. In The Structure and Properties of Porous Materials; Everett, D. H.; Stone, F. S., Eds.; Butterworths: London, **1958**; pp 68–94.
42. Haslam, E. *J. Soc. Leather Technol. Chem.* **1997**, *81*, 45.
43. Chandrasekaran, B.; Rao, J. R.; Sreeran, K. J.; Nair, B. U.; Ramasami, T. *J. Sci. Ind. Res.* **1999**, *58*, 1.
44. Fathima, N. N.; Rao, J. R.; Nair, B. U. *J. Soc. Leather Technol. Chem.* **2003**, *87*, 227.
45. Bull, H. B. *J. Am. Chem. Soc.* **1944**, *66*, 1499.
46. Dole, M.; McLaren, A. D. *J. Am. Chem. Soc.* **1947**, *69*, 651.
47. Kozlov, P. V.; Burdygina, G. I. *Polymer* **1983**, *24*, 651.